

# **Modelling and Fixed Step Simulation of a Turbo Charged Diesel Engine**

**Master's thesis**  
performed in **Vehicular Systems**

by  
**Jesper Ritzén**

Reg nr: LiTH-isy-ex-3442-2003

13th June 2003



# **Modelling and Fixed Step Simulation of a Turbo Charged Diesel Engine**

**Master's thesis**

performed in **Vehicular Systems,**  
**Dept. of Electrical Engineering**  
at **Linköpings universitet**

by **Jesper Ritzén**

Reg nr: LiTH-ISY-EX-3442-2003

Supervisor: **Mattias Nyberg, PhD**

Scania CV AB

**David Elfvik, Msc**

Scania CV AB

**Jonas Biteus, Msc**

Linköpings universitet

Examiner: **Assistant professor Lars Eriksson**

Linköpings Universitet

Linköping, 13th June 2003





**Avdelning, Institution**  
Division, Department  
Vehicular Systems,  
Dept. of Electrical Engineering  
581 83 Linköping

**Datum**  
Date  
13th June 2003

**Språk**

Language

- Svenska/Swedish  
 Engelska/English

\_\_\_\_\_

**Rapporttyp**

Report category

- Licentiatavhandling  
 Examensarbete  
 C-uppsats  
 D-uppsats  
 Övrig rapport  
 \_\_\_\_\_

**ISBN**

—

**ISRN**

LITH-ISY-EX-3442-2003

**Serietitel och serienummer**

Title of series, numbering

**ISSN**

—

**URL för elektronisk version**

<http://www.vehicular.isy.liu.se>  
<http://www.ep.liu.se/exjobb/isy/2003/3442/>

**Titel** Modellering och simulering med fast steglängd av en turboladdad dieselmotor

**Title** Modelling and Fixed Step Simulation of a Turbo Charged Diesel Engine

**Författare** Jesper Ritzén

**Author**

**Sammanfattning**

Abstract

Having an engine model that is accurate but not too complicated is desirable when working with on-board diagnosis or engine control. In this thesis a four state mean value model is introduced. To make the model usable in an on-line automotive application it is discrete and simulated with a fixed step size solver. Modelling is done with simplicity as main object. Some simple static models are also presented.

To validate the model measuring is carried out in a Scania R124LB truck with a 12 liter six-cylinder turbo charged diesel engine. In general, for this relatively simple model, the mean errors must be considered low. The inlet manifold pressure mean error during highway driving is 3.4%.

**Nyckelord**

**Keywords** mean value engine model, manifold pressures, fixed step simulation



## **Abstract**

Having an engine model that is accurate but not too complicated is desirable when working with on-board diagnosis or engine control. In this thesis a four state mean value model is introduced. To make the model usable in an on-line automotive application it is discrete and simulated with a fixed step size solver. Modelling is done with simplicity as main object. Some simple static models are also presented.

To validate the model measuring is carried out in a Scania R124LB truck with a 12 liter six-cylinder turbo charged diesel engine. In general, for this relatively simple model, the mean errors must be considered low. The inlet manifold pressure mean error during highway driving is 3.4%.

**Keywords:** mean value engine model, manifold pressures, fixed step simulation

## Preface

This master's thesis has been performed for Scania at the division of Engine Software and OBD (NEE) during the spring of 2003.

### Thesis outline

**Chapter 1, Introduction** Introduction to the thesis.

**Chapter 2, Experimental setup** A presentation of the test vehicle and where and how different variables are measured.

**Chapter 3, Engine modelling** How the engine is modelled.

**Chapter 4, Static models** Some different static models made from simplifications in the engine model.

**Chapter 5, Simulation** How the model was simulated and difficulties with fixed step size simulation.

**Chapter 6, Tuning** How the model was tuned against measured data

**Chapter 7, Validation** Validation of the engine model.

**Chapter 8, Conclusions and Future Work** Discussion about the results presented in this thesis, and future work that can be done to improve the model.

### Acknowledgments

I would like to thank my supervisors at Scania, David Elfvik and Mattias Nyberg and my supervisor at Linköpings universitet, Jonas Biteus for their support and encouragement. I would also like to thank Ola Härkegård at Linköpings universitet for helping me with simulation problems and all the people at Scania who have helped and inspired me.

*Jesper Ritzén*  
Södertälje, June 2003

# Contents

<b>Abstract</b>	<b>v</b>
<b>Preface and Acknowledgment</b>	<b>vi</b>
<b>1 Introduction</b>	<b>1</b>
<b>2 Experimental setup</b>	<b>3</b>
2.1 Experimental setup, introduction . . . . .	3
2.2 Temperatures . . . . .	3
2.3 Pressures . . . . .	4
2.4 Turbine speed . . . . .	6
2.5 Technical problems . . . . .	6
<b>3 Engine modelling</b>	<b>9</b>
3.1 Engine model . . . . .	9
3.2 Inlet manifold . . . . .	9
3.3 Volumetric efficiency . . . . .	11
3.4 Exhaust manifold . . . . .	11
3.4.1 Exhaust gas temperature . . . . .	12
3.5 Exhaust system . . . . .	13
3.6 Turbocharger . . . . .	13
3.6.1 Compressor model . . . . .	13
3.6.2 Turbine model . . . . .	14
3.7 Summary, engine model . . . . .	14
<b>4 Static models</b>	<b>15</b>
4.1 Static model, inlet manifold . . . . .	15
4.2 Static model, exhaust manifold . . . . .	17
4.3 Summary, static models . . . . .	17
<b>5 Simulation</b>	<b>19</b>
5.1 Fixed step simulation . . . . .	19
5.2 Choosing discrete time integrators . . . . .	19
5.3 Simulation performance . . . . .	21

<b>6</b>	<b>Tuning</b>	<b>25</b>
6.1	Constants . . . . .	25
6.2	Flow and efficiency maps . . . . .	25
<b>7</b>	<b>Validation</b>	<b>27</b>
7.1	Validation method . . . . .	27
7.2	Inlet manifold pressure validation . . . . .	28
7.3	Exhaust manifold pressure validation . . . . .	28
7.4	Exhaust manifold temperature validation . . . . .	28
7.5	Exhaust system pressure validation . . . . .	31
7.6	Exhaust system temperature validation . . . . .	32
7.7	Turbine speed validation . . . . .	32
7.8	Statistical analysis . . . . .	33
7.9	Summary . . . . .	34
<b>8</b>	<b>Conclusions and future work</b>	<b>35</b>
8.1	Conclusions . . . . .	35
8.1.1	Model performance . . . . .	35
8.1.2	Simulation performance . . . . .	35
8.2	Future work . . . . .	36
	<b>References</b>	<b>37</b>
	<b>Notation</b>	<b>39</b>

# Chapter 1

## Introduction

### Background

Legislative restrictions are getting more and more strict on manufacturers of heavy duty trucks. From 2005 all trucks sold in the EU must have an On Board Diagnostics (OBD) system. The aim of the OBD system is to make sure emission restrictions are kept, even when the vehicle is on duty. New methods are needed to meet these requirements and building models is a way of achieving them. Models can also be used for engine control and also replace sensors, and the thereby lower costs.

### Objectives

The objective of this thesis is to create a mean value model of a turbo charged diesel engine which can be simulated with a fixed step size solver. The model should be accurate and as simple as possible. The main objective when building the mean value model has been to keep it simple. A model that is to be used in an on-line automotive application must combine accuracy with simplicity and being reliable without being too complex. Validation is to be made in a Scania truck.

### Methods

The model is built and simulated with Matlab/Simulink from Mathworks. Data for model building and validation is collected from a Scania R124LB truck with a 12 liter, 6 cylinder turbo charged diesel engine.

## **Target group**

The thesis is aimed for engineers and students with basic knowledge in vehicular systems.

## Chapter 2

# Experimental setup

To validate the model, measuring is carried out in a research vehicle. Sensor locations are chosen and sensors are installed. The sensor signals are filtered and amplified and connected to a measuring interface.

### 2.1 Experimental setup, introduction

The research vehicle used is a Scania R124LB 6×2 truck with a 12 liter six-cylinder turbo charged diesel engine, loaded to a total weight of 22700 kg, see figure 2.1.

A lot of time has been devoted to choosing sensors and solving technical problems to make the measurements working, see section 2.5 for technical problems. A view of the experimental setup is seen in figure 2.2. A view of where the sensors are placed on the engine is shown in figure 2.3. Measuring is done with a laptop with Vision software connected to an interface, both from Accurate Technologies Inc, ATI. The interface can communicate with the engine control system used in Scania trucks, S6. It has also analog inputs and inputs for thermoelements, type K. A complete list of the sensors installed is seen in table 2.1.

### 2.2 Temperatures

Temperatures are measured by thermoelements, type K. Where the temperatures are high, i.e. after combustion, the thermoelements are encapsulated. This means that the heating and cooling effects in the encapsulation must be considered when validation is made. The thermoelements are connected directly to the Vision interface. K-elements are chosen because the ATI interface has K-element inputs and because they are considered accurate enough for this kind of measurement. The temperature range is  $-40$  to  $1200$  °C with



**Figure 2.1:** The research vehicle, a Scania R124LB 6×2 420 hp, and the author.

an accuracy of  $\pm 2.5^{\circ}C$  when the temperature is between  $-40$  and  $333^{\circ}C$  and  $\pm 0.75\%$  of the absolute temperature when the temperature is between  $333$  and  $1200^{\circ}C$ .

## 2.3 Pressures

Pressure is measured by three different types of sensors: Gould-Statham pressure sensors for pressures where the temperatures are lower; Kistler pressure sensors for pressures where the temperatures are higher and a Dynisco sensor for ambient pressure. The accuracy of the pressure sensors is less than  $\pm 0.10\%$  of the calibrated measuring range for the Gould-Statham sensors and  $\pm 0.11\%$  for the Dynisco sensor. The accuracy of the Kistler sensors is  $\pm 0.3\%$  off the calibrated measuring range. To protect the sensors from the heat around the engine, thin pipes have been installed between the pressure sensors and their respective point of measuring. Signals from the Gould-Statham pressure sensors and the Dynisco sensors are filtered and amplified by a Scania EMC90 interface which is connected to the Vision interface. The Kistler sensors are amplified by Kistler amplifiers and connected to the Vision interface.

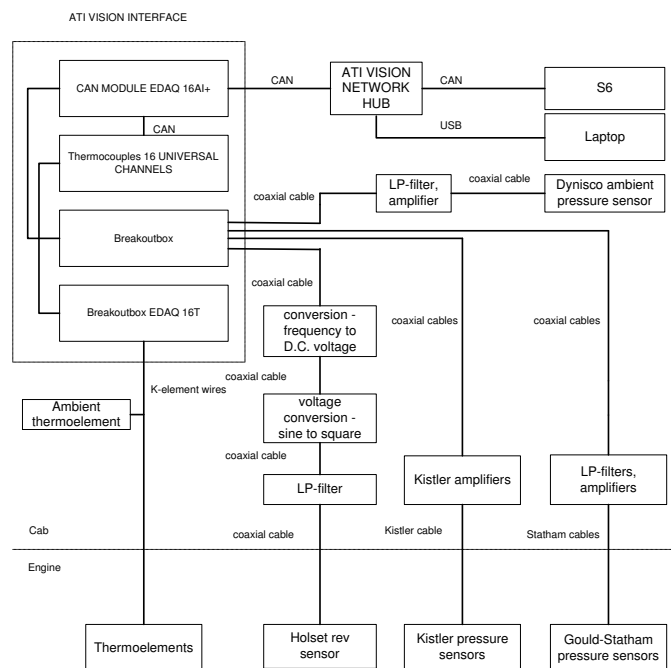


**Figure 2.2:** The experimental setup.

## 2.4 Turbine speed

To measure the turbine speed a Holset induction revolution sensor is used. A magnetic nut is installed on the turbine shaft and the magnetic field which is generated when the shaft rotates induces a voltage in the sensor. The signal from the sensor is very noisy and must be low pass filtered. The filtered signal is then converted from sine wave to square wave to make it easier to detect the frequency of the signal. The square wave signal is then converted to a direct current voltage signal.

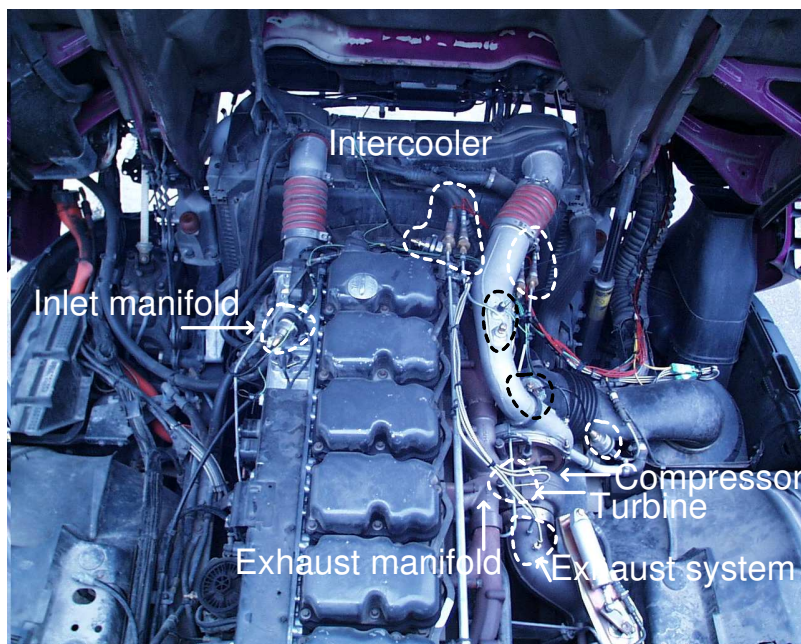


**Figure 2.3:** The research engine. Dashed areas show where sensors and points of measuring are placed.

## 2.5 Technical problems

Some technical problems occurred when working with the experimental setup. Here is a list of some of the major ones.

**Turbine speed sensor signal** The signal from the Holset rev sensor is very noisy, and it was hard finding the right way of converting it to a direct current signal.

**Pressure sensors** Finding suitable pressure sensors and protecting them from the heat around the engine.

**Pressure sensor pipes** How to draw the thin pipes between the pressure sensors and their respective point of measuring, without making them too long, and not too short so the sensors would be damaged by the heat from the engine.

**Exhaust system pressure** The exhaust system pressure sensor, measuring the pressure after the turbine, has occasionally been covered by dirt and stopped working properly.

**Table 2.1:** Measured variables.

Temperature	Description	Sensor
$T_{amb}$	Ambient temperature [K]	Thermoelement, type K
$T_{cmp_{in}}$	Temperature before compressor [K]	Thermoelement, type K
$T_{cmp_{out}}$	Temperature after compressor [K]	Thermoelement, type K
$T_{intercooler}$	Temperature after intercooler [K]	Thermoelement, type K
$T_{im}$	Inlet manifold temperature [K]	Thermoelement, type K
$T_{em_1}$	Exhaust manifold temperature 1 [K]	Thermoelement, type K
$T_{em_2}$	Exhaust manifold temperature 2 [K]	Thermoelement, type K
$T_{es}$	Temperature after turbine [K]	Thermoelement, type K
$T_{eng}$	Cooling water temperature [K]	Thermoelement, type K
<b>Pressure</b>		
$p_{amb}$	Ambient pressure [bar]	Dynisco PT310JA-15
$p_{cmp_{in}}$	Pressure before compressor [bar]	Gould-Statham PG , 3 bar
$p_{cmp_{out}}$	Pressure after compressor [bar]	Kistler 4045A5, 5 bar
$p_{intercooler}$	Pressure after intercooler [bar]	Gould-Statham PG , 6 bar
$p_{im}$	Inlet manifold pressure [bar]	Gould-Statham PG , 6 bar
$p_{em_1}$	Exhaust manifold pressure 1 [bar]	Kistler 4045A10, 10 bar
$p_{em_2}$	Exhaust manifold pressure 2 [bar]	Kistler 4045A10, 10 bar
$p_{es}$	Exhaust system pressure [bar]	Kistler 4075A10, 10 bar
<b>Other</b>		
$n_{tb}$	Turbine speed [rpm]	Holset ind. rev. sensor
$v_{vehicle}$	Vehicle speed [km/h]	From S6
$n_{eng}$	Engine speed [rpm]	From S6
$\delta$	Injected fuel [mg/stroke]	From S6



## Chapter 3

# Engine modelling

This chapter describes the modelling of the air path of a six cylinder 12 liter turbo charged diesel engine. The model is a Mean Value Engine Model, MVEM, which means that variables and signals that are considered are averaged over one or several cycles.

### 3.1 Engine model

The main objective when building the mean value model has been to keep it simple. A model that is to be used in an automotive on-line application must combine accuracy with simplicity, being reliable without being too complex. The modelling done in this thesis is based on the previous work [1], [2] and [3], but made in a simpler way. The exhaust temperature model is taken from [5]. The model has four states: inlet manifold pressure, exhaust manifold pressure, exhaust system pressure and turbine speed. All control volumes, i.e. inlet manifold, exhaust manifold and exhaust system are considered ideal in terms of pressure, temperature and heat transfer. The heat transfer is assumed zero. The inlet manifold temperature is not modelled and considered as an input, since it is available from Scania's engine control system, S6. Specific heat capacity at constant pressure,  $c_p$ , and volume,  $c_v$ , are modelled as constants, with one value before the combustion and another one after. See figures 3.1 and 3.2 for a view of the model.

### 3.2 Inlet manifold

The inlet manifold is considered ideal in terms of pressure and temperature. If the inlet manifold is considered as a control volume, the ideal gas law

$$p = \frac{mRT}{V} \quad (3.1)$$

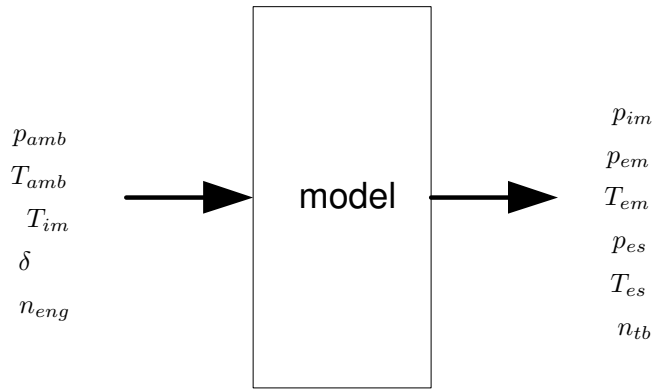


**Figure 3.1:** Variables  $p_{amb}$ ,  $T_{amb}$ ,  $T_{im}$ ,  $\delta$  and  $n_{eng}$  are inputs to the model. Variables  $p_{im}$ ,  $p_{em}$ ,  $p_{es}$ ,  $T_{em}$ ,  $T_{es}$  and  $n_{tb}$  are outputs from the model.

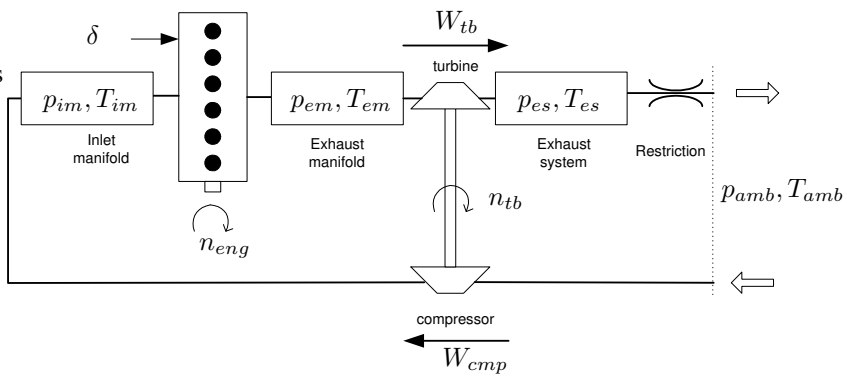


**Figure 3.2:** A view of the model structure.

can be used to derive the change of pressure in the inlet manifold. By differentiating 3.1

$$\dot{p} = \frac{\dot{m}RT}{V} + \frac{mR\dot{T}}{V} \quad (3.2)$$

and assuming that the temperature varies slowly

$$\dot{T} = 0 \quad (3.3)$$

we get

$$\dot{p}_{im} = \frac{R_i T_{im}}{V_{im}} (W_{im_{In}} - W_{im_{Out}}), \quad (3.4)$$

where  $W_{im_{In}}$  is the mass flow into the inlet manifold and  $W_{im_{Out}}$  the mass flow out of the inlet manifold. The mass flow into the inlet manifold is considered to be the massflow trough the compressor, therefore

$$W_{im_{In}} = W_{cmp}. \quad (3.5)$$

The mass flow out of the inlet manifold is considered to be the mass flow into the cylinders, which is modelled as

$$W_{im_{Out}} = W_{eng_{In}} \quad (3.6)$$

$$W_{eng_{In}} = \eta_{vol} \frac{p_{im} V_d N_{cyl} n_{eng}}{60 N_r R_{im} T_{im}}, \quad (3.7)$$

where  $\eta_{vol}$  is the volumetric efficiency,  $V_d$  the displacement volume,  $N_{cyl}$  the number of cylinder,  $n_{eng}$  the engine speed,  $N_r$  the number of revolutions per cycle,  $R_{im}$  the gas constant and  $T_{im}$  the inlet manifold temperature.

### 3.3 Volumetric efficiency

The volumetric efficiency is the efficiency of the engine induction process. It is defined as the actual volume flow rate of air divided by the theoretical volume flow rate of air displaced by the pistons. It is modelled as

$$\eta_{vol} = f_{\eta_{vol}}(n_{eng}), \quad (3.8)$$

where  $f_{\eta_{vol}}$  is a look-up table constructed from engine data.

### 3.4 Exhaust manifold

The exhaust manifold is as the inlet manifold considered ideal in terms of pressure and temperature, (3.1), (3.2) and (3.3) gives

$$\dot{p}_{em} = \frac{R_e T_{em}}{V_{em}} (W_{em_{In}} - W_{em_{Out}}). \quad (3.9)$$

The mass flow out of the exhaust manifold is considered to be the mass flow through the turbine

$$W_{emOut} = W_{tb}. \quad (3.10)$$

The mass flow out of the engine is the mass flow into the exhaust manifold

$$W_{emIn} = W_{engOut}. \quad (3.11)$$

The mass flow out of the engine equals the sum of the mass flow into the cylinders and the mass flow of injected fuel

$$W_{engOut} = W_{engIn} + W_{fuel}, \quad (3.12)$$

where

$$W_{fuel} = \frac{\delta n_{eng} N_{cyl}}{60 N_r}, \quad (3.13)$$

where  $\delta$  is the amount of injected fuel per stroke.

### 3.4.1 Exhaust gas temperature

The exhaust temperature is modelled as an ideal Otto cycle and is taken from [5]

$$T_{em} = T_1 \left( \frac{p_{em}}{p_{im}} \right)^{\frac{\gamma_e - 1}{\gamma_e}} \left( 1 + \frac{q_{in}}{c_v T_1 r_c^{\gamma_e - 1}} \right)^{\frac{1}{\gamma_e}}, \quad (3.14)$$

where  $\gamma_e$  is the ratio of heat capacities after the combustion. The specific energy of the charge per mass is

$$q_{in} = \frac{W_{fuel} q_{HV}}{W_{engIn} + W_{fuel}} (1 - x_r). \quad (3.15)$$

The residual gas fraction is

$$x_r = \frac{1}{r_c} \left( \frac{p_{em}}{p_{im}} \right)^{\frac{1}{\gamma_e}} \left( 1 + \frac{q_{in}}{c_v T_1 r_c^{\gamma_e - 1}} \right)^{-\frac{1}{\gamma_e}}, \quad (3.16)$$

where  $r_c$  is the compression ratio and  $c_v$  the specific heat capacity at constant volume. The model is complete with

$$T_1 = x_r T_{em} + (1 - x_r) T_{im}. \quad (3.17)$$

This model is not really suitable for fixed step solvers because  $q_{in}$  and  $T_1$  are obtained by solving a nonlinear equation system at each time step. The equation system, defined by the equations (3.15), (3.16) and (3.17), is solved by the fixed step discrete solver available in Matlab/Simulink. The model is chosen because it shows low errors during validation and is not as complicated as the Seliger cycle model presented in [5].

### 3.5 Exhaust system

As above the dynamics is

$$\dot{p}_{es} = \frac{R_e T_{es}}{V_{es}} (W_{esIn} - W_{esOut}). \quad (3.18)$$

The mass flow into the exhaust system equals the flow through the turbine

$$W_{esIn} = W_{tb}. \quad (3.19)$$

The exhaust system is modelled as a quadratic restriction

$$W_{esOut}^2 = \frac{k_{es} R_e T_{es}}{p_{es}} (p_{es} - p_{amb}), \quad (3.20)$$

where  $k_{es}$  is the exhaust system restriction constant. The exhaust system temperature is modelled as

$$T_{es} = T_{tbOut}, \quad (3.21)$$

where  $T_{tbOut}$  is the temperature out from the turbine.

### 3.6 Turbocharger

The turbocharger is modelled as described in [2]. The turbine and compressor maps described below are extrapolated from data provided by the turbocharger manufacturer. Newton's second law

$$J\dot{\omega} = M \quad (3.22)$$

Gives that the turbine speed is described by

$$\dot{\omega}_{tb} = \frac{1}{J_{tb}} (M_{tb} - M_{cmp}), \quad (3.23)$$

where  $J_{tb}$  is the mechanical inertia of the turbocharger,  $M_{tb}$  is the torque produced by the turbine and  $M_{cmp}$  is the torque produced by the compressor.

#### 3.6.1 Compressor model

The compressor is described by two different maps, the flow map,  $f_{W_{cmp}}$ , and the efficiency map,  $f_{\eta_{cmp}}$ . The mass flow and efficiency of the compressor is modelled as

$$W_{cmp} = f_{W_{cmp}} \left( \frac{p_{im}}{p_{amb}}, n_{tb} \right) \frac{p_{im}}{\sqrt{T_{amb}}} \quad (3.24)$$

$$\eta_{cmp} = f_{\eta_{cmp}} \left( \frac{p_{im}}{p_{amb}}, n_{tb} \right). \quad (3.25)$$

The torque produced by the compressor is

$$M_{cmp} = \frac{W_{cmp} c_{p_i} T_{amb}}{\eta_{cmp} \omega_{tb}} \left( \left( \frac{p_{im}}{p_{amb}} \right)^{\frac{\gamma_i - 1}{\gamma_i}} - 1 \right), \quad (3.26)$$

where  $c_{p_i}$  is the specific heat capacity at constant pressure before combustion and  $\gamma_i$  the ratio of heat capacities before the combustion.

### 3.6.2 Turbine model

As for the compressor, the turbine is described by two maps,  $f_{W_{tb}}$  and  $f_{\eta_{tb}}$ . The mass flow and the efficiency of the turbine is modelled as

$$W_{tb} = f_{W_{tb}} \left( \frac{p_{em}}{p_{es}}, n_{tb} \right) \frac{p_{em}}{\sqrt{T_{em}}} \quad (3.27)$$

$$\eta_{tb} = f_{\eta_{tb}} \left( \frac{p_{em}}{p_{es}}, n_{tb} \right). \quad (3.28)$$

The temperature out from the turbine is modelled as

$$T_{tb_{out}} = \left( 1 + \eta_{tb} \left( \left( \frac{p_{em}}{p_{es}} \right)^{\frac{1 - \gamma_e}{\gamma_e}} - 1 \right) \right) T_{tb_{in}}. \quad (3.29)$$

The torque produced by the compressor is

$$M_{tb} = \frac{W_{tb} c_{p_e} T_{em} \eta_{tb}}{\omega_{tb}} \left( 1 - \left( \frac{p_{em}}{p_{es}} \right)^{\frac{1 - \gamma_e}{\gamma_e}} \right), \quad (3.30)$$

where  $c_{p_e}$  is the specific heat capacity at constant pressure after combustion.

## 3.7 Summary, engine model

The engine model, which will be referred to as the four state model, has four state equations

$$\dot{p}_{im} = \frac{R_i T_{im}}{V_{im}} (W_{im_{In}} - W_{im_{Out}}) \quad (3.31)$$

$$\dot{p}_{em} = \frac{R_e T_{em}}{V_{em}} (W_{em_{In}} - W_{em_{Out}}) \quad (3.32)$$

$$\dot{p}_{es} = \frac{R_e T_{es}}{V_{es}} (W_{es_{In}} - W_{es_{Out}}) \quad (3.33)$$

$$\dot{\omega}_{tb} = \frac{1}{J_{tb}} (M_{tb} - M_{cmp}) \quad (3.34)$$

The variables  $p_{amb}$ ,  $T_{amb}$ ,  $T_{im}$ ,  $\delta$  and  $n_{eng}$  are inputs to the model.

## Chapter 4

# Static models

To have non complex static models that are easy to calculate would be very useful if they are accurate enough. Two different static models, which are derived from simplifications made in the engine model, are discussed in this chapter. The static models are not validated in this thesis because more work has to be done before a proper validation could be useful. They are presented here as an example of how static models can be achieved. The basic principle is to neglect dynamics. It is seen that situations occur where the desired pressure is an input to a look-up table. It is then necessary to invert the look-up table to get a static relationship for the desired pressure. An example: Assume that  $x$  and  $y$  are known variables and  $p$  is the pressure. After neglecting pressure dynamics,  $\dot{p} = 0$ , we have

$$x = f_{map}(p, y).$$

Inverting the map yields

$$p = \tilde{f}_{map}(x, y),$$

and a static expression describing the pressure is achieved.

### 4.1 Static model, inlet manifold

If the inlet manifold dynamics is neglected, i.e.  $\dot{p}_{im} = 0$ , (3.4) becomes

$$W_{imIn} = W_{imOut}. \quad (4.1)$$

With (3.5), (3.6), (3.7) and (3.24), expression (4.1) becomes

$$\frac{p_{im}}{p_{amb}} = \frac{60N_r R_i}{\eta_{vol} V_d N_{cyl}} \frac{T_{im}}{\sqrt{T_{amb} n_{eng}}} f_{W_{emp}} \left( \frac{p_{im}}{p_{amb}}, n_{tb} \right). \quad (4.2)$$

Let

$$z_1 = \left( \frac{60N_r R_i}{\eta_{vol} V_d N_{cyl}} \frac{T_{im}}{\sqrt{T_{amb} n_{eng}}} \right)^{-1}, \quad (4.3)$$

then (4.1) becomes

$$z_1 = f_{W_{cmp}} \left( \frac{p_{im}}{p_{amb}}, n_{tb} \right) \frac{p_{amb}}{p_{im}}, \quad (4.4)$$

which can be simplified as

$$z_1 = \tilde{f}_{W_{cmp}} \left( \frac{p_{im}}{p_{amb}}, n_{tb} \right), \quad (4.5)$$

due to the fact that  $\frac{p_{im}}{p_{amb}}$  is included in the look-up table. It can be rewritten as

$$p_{im} = f \left( z_1, n_{tb} \right) p_{amb}, \quad (4.6)$$

with a new map  $f$ . An example plot of the static model for  $p_{im}$  compared to the four state engine model  $p_{im}$ , described in section 3.7, is seen in figure 4.1. Note that there are not as much oscillations in the static model for  $p_{im}$  compared to the four state model  $p_{im}$ .

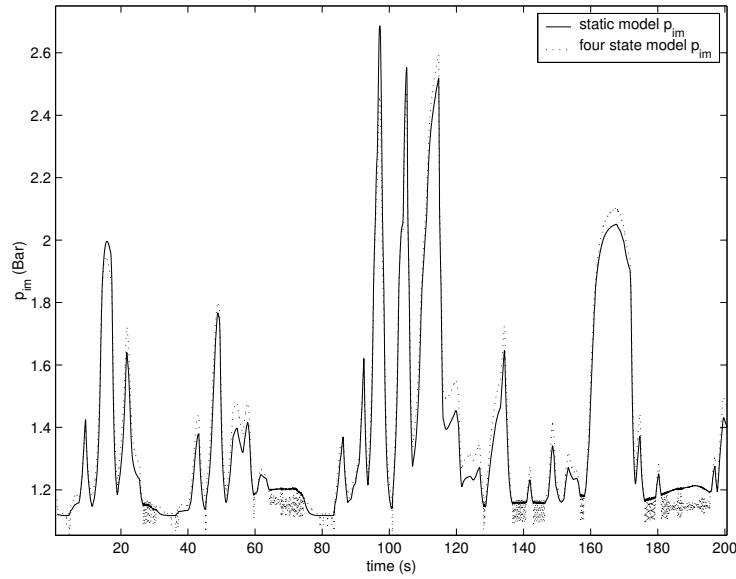


**Figure 4.1:** An example plot of  $p_{im}$  from the four state engine model and the static model  $p_{im}$ .

## 4.2 Static model, exhaust manifold

Neglecting the exhaust manifold dynamics yields a similar case to the one above. No dynamics,  $\dot{p}_{em} = 0$  and (3.9) gives

$$W_{emIn} = W_{emOut}. \quad (4.7)$$

With (3.10), (3.11) and (3.27) it yields

$$W_{engOut} = f_{W_{tb}} \left( \frac{p_{em}}{p_{es}}, n_{tb} \right) \frac{p_{em}}{\sqrt{T_{em}}}. \quad (4.8)$$

Let

$$z_2 = \frac{W_{engOut} \sqrt{T_{em}}}{p_{es}}, \quad (4.9)$$

then (4.7) becomes

$$z_2 = f_{W_{tb}} \left( \frac{p_{em}}{p_{es}}, n_{tb} \right) \frac{p_{em}}{p_{es}}, \quad (4.10)$$

which can be simplified as

$$z_2 = \tilde{f}_{W_{tb}} \left( \frac{p_{em}}{p_{es}}, n_{tb} \right), \quad (4.11)$$

due to the fact that  $\frac{p_{em}}{p_{es}}$  is included in the look-up table. It can be written as

$$p_{em} = g \left( z_2, n_{tb} \right) p_{es}, \quad (4.12)$$

with a new map  $g$ .

## 4.3 Summary, static models

The static models could be a way to achieve models that are accurate and relatively non complex. More work has to be done before a proper validation could be useful.



## Chapter 5

# Simulation

When simulating a model, it is preferable to use a variable step solver. The progression of a simulation often changes between fast and slow variations and therefore it is inefficient to use a fixed step solver. Also, if simulation is done with a too large fixed step size, the simulation gets unstable. But if the model is to be used in an on-line automotive application it must, as said in chapter 1, be simulated with a fixed step solver. The reason to this is that it is important to know exactly how much computing power a function needs. How the simulation is done and difficulties with fixed step size simulation is described in this chapter.

### 5.1 Fixed step simulation

Matlab Simulink from Mathworks is used for simulations. If the model is to be used in an on-line automotive application it must be easy to calculate as the computing power in the vehicle is limited. Therefore it is necessary that the model can be run with a fixed step solver with a fairly long fixed step size. To auto-generate code from the Simulink model it is also necessary to have a discrete model, i.e. no continuous states. The maximum step size, where a model becomes unstable, is determined by its structure. There is no theoretical method how to calculate the maximum fixed step size for non linear models. Testing and simulating is the only way of finding the maximum fixed step size.

### 5.2 Choosing discrete time integrators

Choosing the right type of discrete time integrators is very crucial for the performance of the model. By changing the discrete-time integration methods the structure of the discrete model description changes. The default integrator

method in Simulink is Forward Euler, where  $1/s$  is approximated by

$$\frac{h}{z-1}, \quad (5.1)$$

where  $h$  is the fixed step size. Another method is Backwards Euler, where  $1/s$  is approximated by

$$\frac{hz}{z-1} \quad (5.2)$$

For stiff problems the Trapezoidal method is useful,  $1/s$  is approximated by

$$\frac{h}{2} \frac{z+1}{z-1} \quad (5.3)$$

The state equations of the model are

$$p_{im} = \frac{1}{s} \frac{R_i T_{im}}{V_{im}} (W_{imIn} - W_{imOut}) \quad (5.4)$$

$$p_{em} = \frac{1}{s} \frac{R_e T_{em}}{V_{em}} (W_{emIn} - W_{emOut}) \quad (5.5)$$

$$p_{es} = \frac{1}{s} \frac{R_e T_{es}}{V_{es}} (W_{esIn} - W_{esOut}) \quad (5.6)$$

$$\omega_{tb} = \frac{1}{s} \frac{1}{J_{tb}} (M_{tb} - M_{cmp}) \quad (5.7)$$

The problem with the Backward Euler and the Trapezoidal method is that they create algebraic loops which require a lot of computing power. An example: Assume that  $u$  is the input and  $x$  is the state of the Backward Euler integration, i.e.

$$x = \frac{hz}{z-1} u \quad (5.8)$$

This can be rewritten as

$$x(t+1) = x(t) + hu(t+1), \quad (5.9)$$

where  $t$  is the discrete time. This means that  $u(t+1)$  is needed to calculate  $x(t+1)$ . If  $u(t+1)$  is a function of  $x(t+1)$ , Backward Euler integration will cause algebraic loops. With the same assumptions as above and integrating with the Trapezoidal method we get

$$x = \frac{h}{2} \frac{z+1}{z-1} u \quad (5.10)$$

This can be rewritten as

$$x(t+1) = x(t) + \frac{h}{2} (u(t+1) + u(t)) \quad (5.11)$$

Again,  $u(t+1)$  is needed to calculate  $x(t+1)$ . Testing is done with different configurations of discrete-time integrators. It is seen that the  $p_{im}$ -state is the only state that can be integrated with the Trapezoidal or Backwards Euler method without causing algebraic loops. Using the Trapezoidal method to integrate the  $p_{im}$ -state noticeably increases the longest possible fixed step size. Therefore the chosen integration methods are the Trapezoidal method for the  $p_{im}$ -state and the Forward Euler method for the other states,  $p_{em}$ ,  $p_{es}$  and  $\omega_{tb}$ .

### 5.3 Simulation performance

The computing power in the vehicle is limited. Therefore it is important that the model can be run with a fairly large fixed step size. To determine the maximum fixed step size of the model, the solution when using a variable step solver is compared to fixed step solver solutions. With a larger step size the mean relative errors become larger because of oscillations in the simulation, see figure 5.1. The figure describes the mean relative error of the exhaust manifold pressure when simulating 100 seconds of city driving. It is seen that the four state model can be simulated with step sizes up to 8 ms. With a larger step size the simulation becomes oscillative and at 15 ms unstable. For an example of oscillations see figure 5.2.

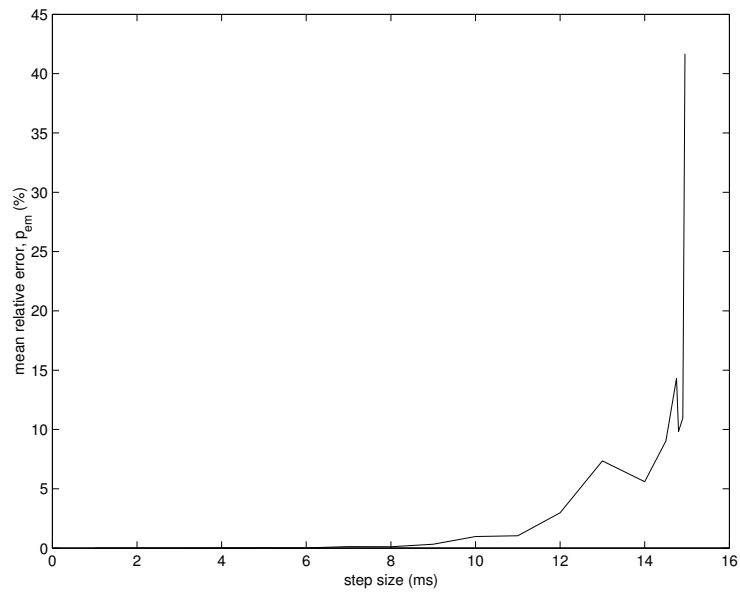


**Figure 5.1:** The mean relative error when comparing variable and fixed step solutions increases when the step size increases. When the step size  $\approx 15$  ms the simulation becomes unstable.

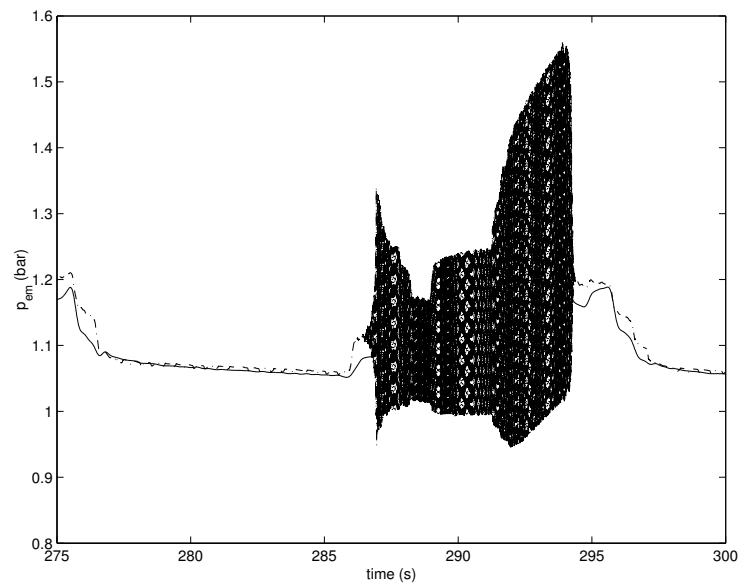


**Figure 5.2:** Example of oscillations when the fixed step size is 12 ms.



## Chapter 6

# Tuning

To get the best performance out of the model it has been tuned against measured data. See table 6.1 for a list of the tuned constants and maps.

### 6.1 Constants

No explicit method has been used when tuning the constants. At first the constants were set to an estimation of their physical value. They were then changed one by one until the best observed model performance was observed. This is not really a good method when tuning, since it is very hard to find the best configuration of constants and hard to know if it is the optimum configuration. Implementation of a script that tunes the model constants automatically against measured data would be preferable. The model has three control volumes  $V_{im}$ ,  $V_{em}$  and  $V_{es}$ . When tuning the model it has been seen that the physically correct size of the volumes does not give the most correct model. E.g., the tuned value of the exhaust system volume is 7000 liters, see table 6.1, which is far greater than the expected size. The reason for this could be that the model is too simple and that too much dynamics is neglected. It could also be that the size of the volumes compensates for other errors in the model. It is hard to know the physically correct values of the moment of inertia of the turbine shaft,  $J_{tb}$ , and the exhaust system restriction constant,  $k_{es}$ . Therefore it is hard to know if the tuned values are close to the physically correct values.

### 6.2 Flow and efficiency maps

The original turbine and compressor flow and efficiency maps have been compared with static measurements done in an engine test cell. The outputs from the original efficiency maps are in general too low, and they are compensated. The flow maps have also been compensated, but without really improving the

validating results. A script that tunes the maps automatically against measured data would probably be helpful.

**Table 6.1:** Tuned variables.

Tuned variable	Description	Value
$V_{im}$	Intake manifold volume [ $dm^3$ ]	1.7
$V_{em}$	Exhaust manifold volume [ $dm^3$ ]	5.0
$V_{es}$	Exhaust system volume [ $dm^3$ ]	7000
$J_{tb}$	Moment of inertia of the turbine shaft [ $Nm.s$ ]	$6.5 \cdot 10^{-4}$
$k_{es}$	Exhaust system restriction constant [ $kg^2/s^2Pa$ ]	50300
$f_{W_{cmp}}$	Compressor flow map [ $kg/s$ ]	$60 \times 60$ look-up table
$f_{\eta_{cmp}}$	Compressor efficiency map [-]	$60 \times 60$ look-up table
$f_{W_{tb}}$	Turbine flow map [ $kg/s$ ]	$60 \times 60$ look-up table
$f_{\eta_{tb}}$	Turbine efficiency map [-]	$60 \times 60$ look-up table

# Chapter 7

## Validation

To validate the model the simulated and the measured quantities are compared. The errors are presented and possible sources of them are discussed in this chapter.

### 7.1 Validation method

The model data used for validation is simulated with a fixed step size of 5 ms. Since no heating or cooling effects are considered in the model all validation is made with measured data where the engine is warm, which in this case means  $T_{eng} > 80^\circ\text{C}$ . Validation is done using three different types of driving:

**City driving** includes many stops and accelerations with speeds ranging up to 60 km/h.

**Highway driving** is done on highway with speeds between 75 and 90 km/h and not much acceleration.

**Mixed driving** is done on smaller roads and with speeds ranging between 30 and 80 km/h including uphill driving.

Four types of errors are considered:

$$\text{mean relative error} = \frac{1}{n} \sum_{i=1}^n \frac{|\hat{x}(t_i) - x(t_i)|}{|x(t_i)|} \quad (7.1)$$

$$\text{maximum relative error} = \max_{1 \leq i \leq n} \frac{|\hat{x}(t_i) - x(t_i)|}{|x(t_i)|} \quad (7.2)$$

$$\text{mean absolute error} = \frac{1}{n} \sum_{i=1}^n |\hat{x}(t_i) - x(t_i)| \quad (7.3)$$

$$\text{maximum absolute error} = \max_{1 \leq i \leq n} |\hat{x}(t_i) - x(t_i)| \quad (7.4)$$

Where  $x(t_i)$  is the measured quantity,  $\hat{x}(t_i)$  is the simulated quantity and  $n$  is the number of samples. A plot of simulated and measured state variables together with  $\delta$ ,  $n_{eng}$  and  $v_{vehicle}$  is shown in figure 7.1.

## 7.2 Inlet manifold pressure validation

The validation data with the largest errors is presented in figure 7.2. The data is taken from the validation file for city driving. It is seen that there is a correlation between the  $p_{im}$  absolute error and the pressure ratio over the compressor,  $\frac{p_{im}}{p_{amb}}$ , and the pressure ratio over the turbine,  $\frac{p_{em}}{p_{es}}$ . High pressure ratios mean high turbine speeds,  $n_{tb}$ . In figure 7.1, when the time is around 110 seconds and 275 seconds, there are particularly large errors. At the same time the turbine speed is too high. It seems like the turbine and compressor flow and efficiency maps are less accurate for high turbine speeds and high pressure ratios. It is also probable that the volumetric efficiency model affects the inlet manifold errors. The turbine flow and efficiency maps are defined for turbine speeds up to 75000 rpm, and for higher speeds extrapolation is made. Therefore, good results can not be expected for high turbine speeds. The inlet manifold mean pressure error is reasonably low, especially for highway driving. See table 7.1 for validation results.

**Table 7.1:** Inlet manifold pressure validation.

Validation	Abs. error (bar)		Rel. error (%)	
	mean	max	mean	max
City driving	0.077	0.64	4.9	30.8
Highway driving	0.053	0.28	3.4	12.8
Mixed driving	0.095	0.52	5.8	25.2

## 7.3 Exhaust manifold pressure validation

The measured exhaust manifold pressure is very noisy and is low pass filtered off-line with a fourth order Butterworth filter with a cutoff frequency of  $10Hz$ . The errors are noticeably lower than the inlet manifold pressure errors. See table 7.2 for validation results.

## 7.4 Exhaust manifold temperature validation

The exhaust manifold temperature is measured with an encapsulated K-element, to protect it from the harsh environment. The heating and cooling effects in the encapsulation mean that the simulated temperature must be low pass filtered to make it comparable to the measured temperature. Filtering is done

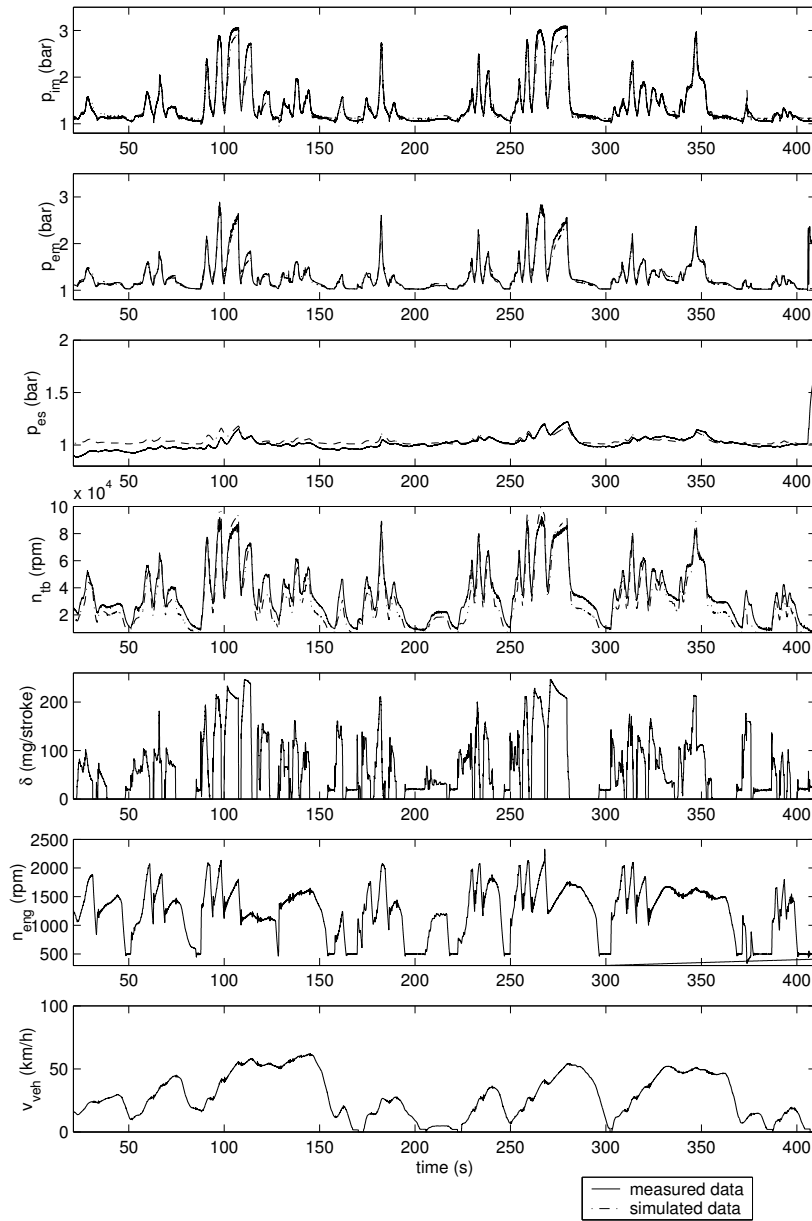


**Figure 7.1:** An example plot of simulated and measured  $p_{im}$ ,  $p_{em}$ ,  $p_{es}$ ,  $n_{tb}$  with  $\delta$ ,  $n_{eng}$  and  $v_{vehicle}$ .

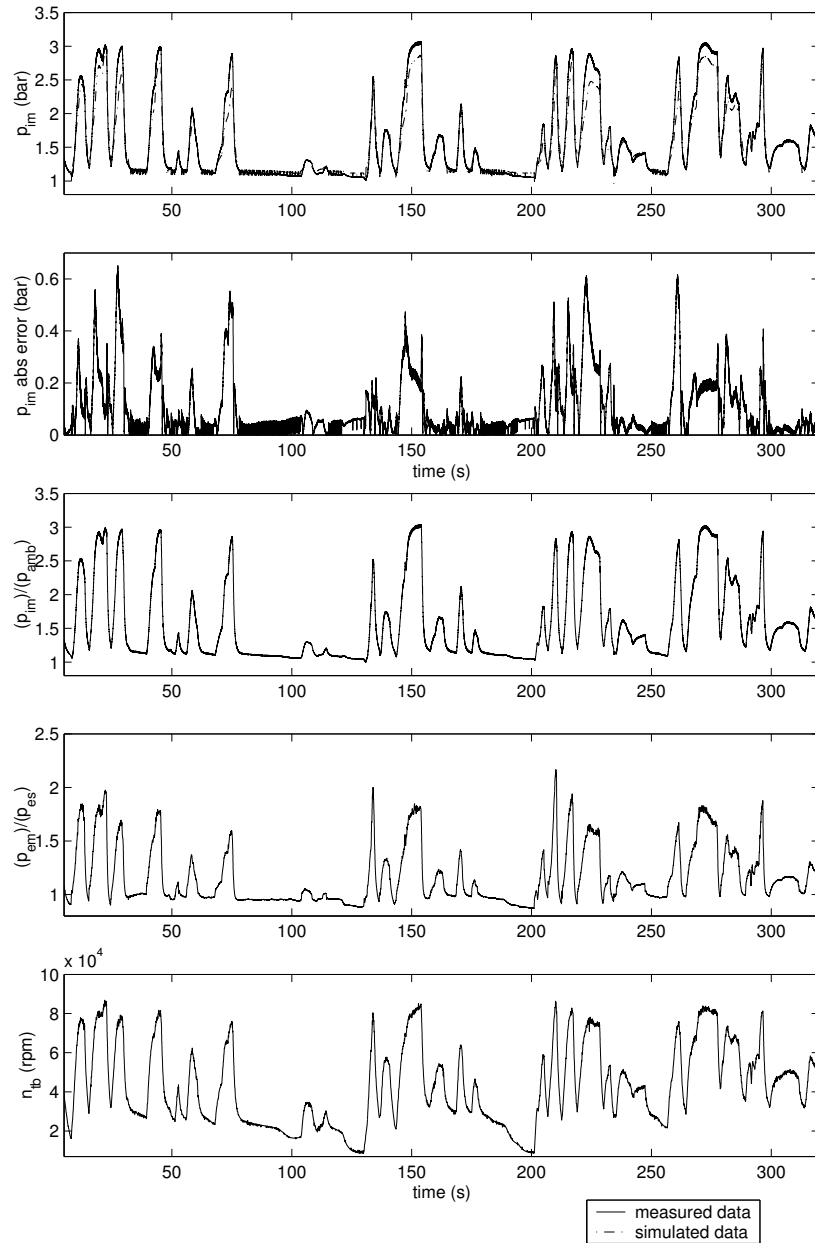


**Figure 7.2:** There is a correlation between the  $p_{im}$  absolute error and the pressure ratios over the compressor,  $\frac{p_{im}}{p_{amb}}$ , and the pressure ratio over the turbine,  $\frac{p_{em}}{p_{es}}$ . High pressure ratios means high turbine speeds,  $n_{tb}$ .

**Table 7.2:** Exhaust manifold pressure validation.

Validation	Abs. error (bar)		Rel. error (%)	
	mean	max	mean	max
City driving	0.039	0.30	2.7	15.1
Highway driving	0.052	0.11	3.8	7.5
Mixed driving	0.039	0.21	2.8	12.4

with a first order Butterworth filter with a cutoff frequency of  $0.035Hz$ . No validation is made here since the simulated signal must be filtered very hard and since validation is made in [5]. See plot in figure 7.3.

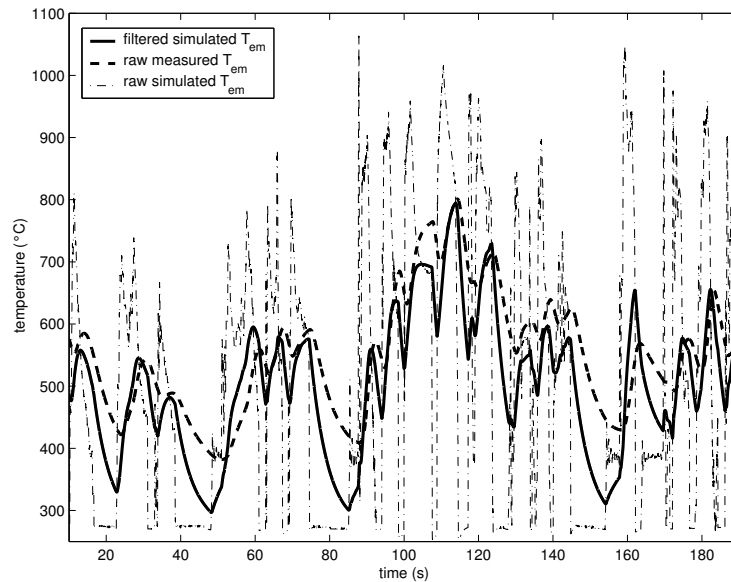


**Figure 7.3:** A plot of filtered simulated  $T_{em}$ , measured raw  $T_{em}$ , and simulated  $T_{em}$ .

## 7.5 Exhaust system pressure validation

The exhaust system pressure is measured after the turbine. The errors are reasonably low and mainly from static conditions. See table 7.3 for validation results.

**Table 7.3:** Exhaust system pressure validation.

Validation	Abs. error (bar)		Rel. error (%)	
	mean	max	mean	max
City driving	0.036	0.10	5.5	9.1
Highway driving	0.027	0.060	2.5	5.4
Mixed driving	0.039	0.085	3.6	7.9

## 7.6 Exhaust system temperature validation

As for the exhaust manifold temperature validation, the simulated exhaust system temperature is low pass filtered. The filter used is the same as for the exhaust manifold temperature. No validation is made, because of the hard filtering, but the measured and filtered simulated  $T_{es}$  seem to correspond. See plot in figure 7.4.

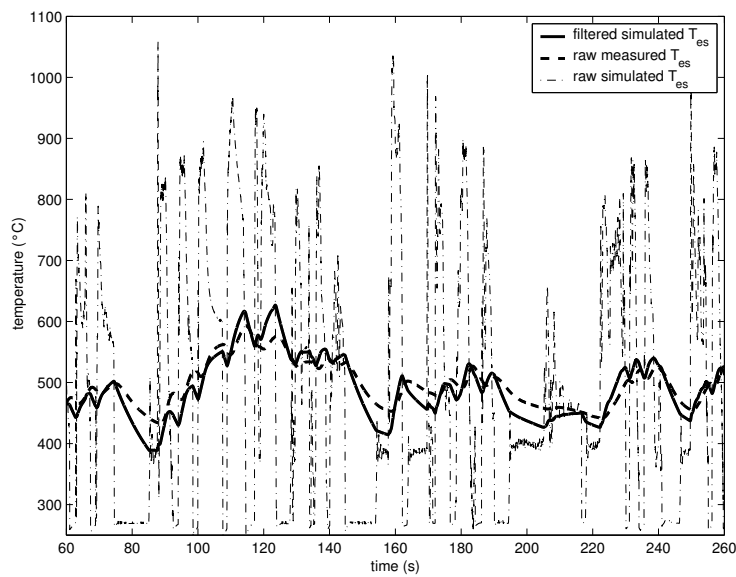


**Figure 7.4:** A plot of filtered simulated  $T_{es}$ , measured raw  $T_{es}$ , and simulated  $T_{es}$ .

## 7.7 Turbine speed validation

The turbine speed errors are seemingly large. As above, more acceleration, i.e. higher turbine speeds lead to larger errors. See table 7.4 for validation

results.

**Table 7.4:** Turbine speed validation.

Validation	Abs. error (rpm)		Rel. error (%)	
	mean	max	mean	max
City driving	6558	17811	15.6	78.2
Highway driving	4480	13200	12.2	45.6
Mixed driving	7488	19017	28.4	75.5

## 7.8 Statistical analysis

Histograms of the error and relative error of the inlet manifold are plotted in figure 7.5 and 7.6. The data comes from 60 minutes of city, mixed and highway driving. The distribution is not too far from symmetrical in relation to zero.

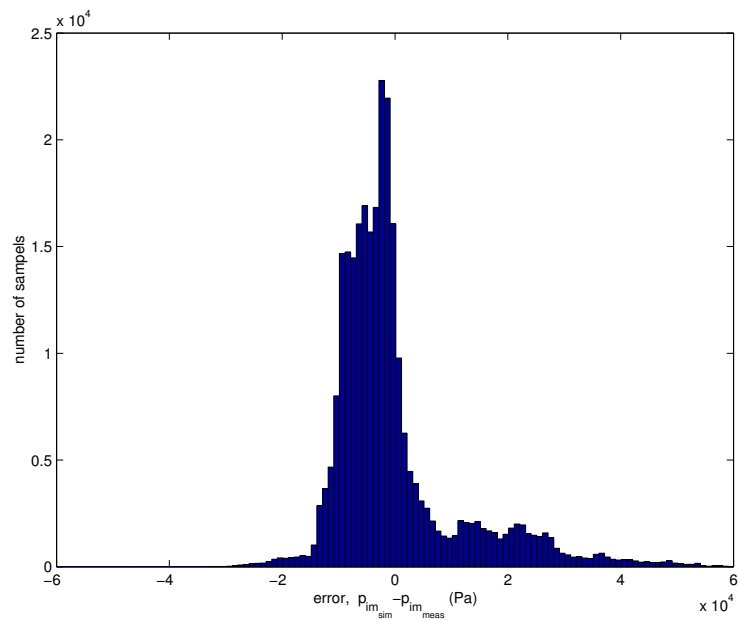


**Figure 7.5:** A histogram of the error of the inlet manifold pressure.

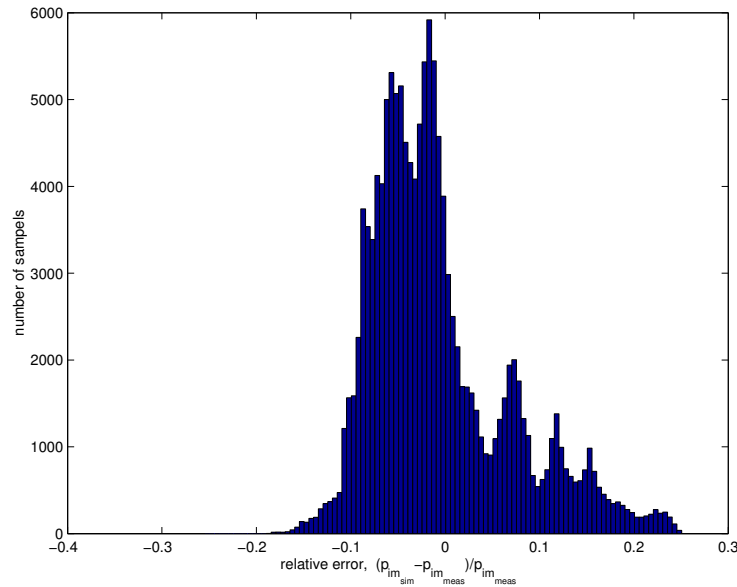


**Figure 7.6:** A histogram of the relative error of the inlet manifold pressure.

## 7.9 Summary

There is a correlation between the  $p_{im}$  absolute error and the pressure ratio over the compressor,  $\frac{p_{im}}{p_{amb}}$ , and the pressure ratio over the turbine,  $\frac{p_{em}}{p_{es}}$ . High pressure ratios mean high turbine speeds,  $n_{tb}$ . It seems like the turbine and compressor flow and efficiency maps are less accurate for high turbine speeds and high pressure ratios. The turbine flow and efficiency maps are defined for turbine speeds up to 75000 rpm, and for higher speed extrapolation is made. It is necessary to get maps that are defined over 75000 rpm in order to get better results. It is also probable that the volumetric efficiency model affects the inlet manifold errors. The inlet manifold mean errors are low, especially for highway driving, where the mean error is 3.4 %. The exhaust manifold pressure shows smaller errors, an explanation could be that the absolute pressures are lower than for the inlet manifold pressure. The exhaust manifold mean error during city driving is 2.7 %. The exhaust system pressure shows fairly small errors and the errors are largest for static conditions. The turbine speed shows larger errors than the other states. In general, for this relatively simple model, the mean errors must be considered low. The errors are slightly higher than in [4], but the models are different and the pressures varies over a wider range in a heavy truck than in a car.

## Chapter 8

# Conclusions and future work

The conclusions made from the model and the simulation performance is discussed in this chapter. Future work that would extend and could improve the model is also presented.

### 8.1 Conclusions

The conclusions made from the performance of the model and the simulation is presented in this section.

#### 8.1.1 Model performance

An attempt has been made to achieve an engine model that is less complicated than earlier models and is possible to simulate with a fixed step size solver. The model shows reasonable low errors. The inlet manifold pressure mean error during highway driving is 3.4 % and the exhaust manifold pressure mean error during city driving is 2.7 %. There is a correlation between the  $p_{im}$  absolute error and the pressure ratio over the compressor,  $\frac{p_{im}}{p_{amb}}$ , and the pressure ratio over the turbine,  $\frac{p_{em}}{p_{es}}$ . The largest source of error seems to be the turbo charger's flow and efficiency maps. It is clear that for high turbine speeds, over 75000 rpm, the inlet and exhaust manifold pressure errors are considerably larger than for turbine speeds under 75000 rpm. The turbine flow and efficiency maps are defined for turbine speeds up to 75000 rpm, and for higher speeds extrapolation is made. To get maps that are defined over 75000 rpm is necessary in order to get better results.

#### 8.1.2 Simulation performance

The model can be simulated with a fixed step size of up to 8 ms without oscillations, which is reasonable. It is desirable to get a model that can be sim-

ulated with a larger fixed step size. The accuracy of the exhaust temperature model is good, but the exhaust temperature is obtained by solving a nonlinear equation system at each time step which slows down the simulation. The attempts to create static models in chapter 3 is a way to achieve small and applicable models that can be simulated with a large fixed step size.

## 8.2 Future work

A lot of work can be done to improve and expand the model. This is a list of the major ones.

**Flow and efficiency maps** The most important issue is getting better flow and efficiency maps. It is crucial if better model performance is to be achieved.

**Automatic tuning** Implementation of a script that tunes the model against measured data.

**Simulation performance** Improve the simulation performance, i.e make the model easier to calculate.

**EGR, VGT, Turbo Compound** Expanding the model with EGR, Exhaust Gas Recirculation, VGT, Variable Geometry Turbo charger and Turbo Compound.

**Static models** The static models could be useful if more work is done.

# References

- [1] D. Elfvik. Modelling of a diesel engine with vgt for control design simulations. Master's thesis IR-RT-EX-0216, Department of Signals, Sensors and Systems, Kungliga tekniska högskolan, Stockholm, Sweden, July 2002.
- [2] L. Guzzela and A. Amstutz. Control of diesel engines. *IEEE Control Systems*, AC-37(7):53–71, October 1998.
- [3] T. Stutte M. Nyberg and V. Wilhelmi. Model based diagnosis of the air path of an automotive diesel engine. In *IFAC Workshop: Advances in Automotive Control*, Karlsruhe, Germany, 2001. IFAC Workshop: Advances in Automotive Control.
- [4] S. Öberg. Identification and improvements of an automotive diesel engine model purposed for model based diagnosis. Master's thesis LiTH-ISY-EX-3161, Department of Electrical Engineering, Linköpings Universitet, Linköping, Sweden, December 2001.
- [5] P. Skogtjärn. Modelling of the exhaust gas temperature for diesel engines. Master's thesis LiTH-ISY-EX-3378, Department of Electrical Engineering, Linköpings Universitet, Linköping, Sweden, December 2002.



# Notation

**Table 8.1:** Symbols used in the report.

Symbol	Value	Description	Unit
$\gamma$	$c_p/c_v$	Ratio of heat capacities	—
$\delta$	Var	Amount of injected fuel	$kg/stroke$
$\eta$	Var	Efficiency	—
$\eta_{vol}$	Var	Volumetric efficiency	—
$c_p$	Con	Specific heat capacity at constant pressure	$J/(kg \cdot K)$
$c_v$	Con	Specific heat capacity at constant volume	$J/(kg \cdot K)$
$R$	$c_p - c_v$	Gas constant	$J/(kg \cdot K)$
$M$	Var	Torque	$Nm$
$n$	Var	Rotational speed	$rpm$
$\omega$	Var	Rotational speed	$\frac{1}{s}$
$N_r$	2	Revolutions per cycle	—
$N_{cyl}$	6	Number of cylinders	—
$p$	Var	Pressure	$Pa$
$\dot{p}$	Var	Change of pressure	$Pa/s$
$q_{HV}$	Con	Heating value	$J/kg$
$q_{in}$	Var	Specific energy content of the charge per unit mass	$J/kg$
$T$	Var	Temperature	$K$
$V$	Var	Volume	$m^3$
$W$	Var	Mass-flow	$kg/s$
$\dot{m}$	Var	Mass-flow	$kg/s$
$x_r$	Var	Residual gas fraction	—
$r_c$	Con	Compression ratio	—
$J$	Con	Moment of inertia	$Nms$
$V_d$	Con	Displacement volume (1 cylinder)	$m^3$
$V_{cyl}$	Con	Cylinder volume (1 cylinder)	$m^3$
$k_{es}$	Con	restriction constant	$kg^2/(s^2 Pa)$
$v_{vehicle}$	Var	Vehicle speed	$km/h$

**Table 8.2:** Abbreviations used in this report.

Abbreviation	Explanation
Con	Constant
Var	Variable
EGR	Exhaust Gas Recirculation
rpm	Revolutions Per Minute
VGT	Variable Geometry Turbine
IC	Intercooler
S6	Scania's engine control system
OBD	On-Board Diagnostics

**Table 8.3:** Indices used in this report.

Index	Explanation
i	Before combustion
e	After combustion
im	Inlet manifold
em	Exhaust manifold
es	Exhaust system
tb	Turbine
cmp	Compressor
eng	Engine
meas	Measured
sim	simulated
amb	Ambient
in	Into the component
out	Out of the component